Journal of Materials Chemistry A

ROYAL SOCIETY OF CHEMISTRY

REVIEW

View Article Online
View Journal | View Issue

Cite this: J. Mater. Chem. A, 2024, 12, 1910

Advancements in radiation resistance and reinforcement strategies of perovskite solar cells in space applications

Zhenghao Huan,[ab] Yifan Zheng,[ab]* Kangpeng Wang,[a] Zicai Shen,[c] Wang Ni,[d] Jifeng Zu[a] and Yuchuan Shao*[ab]

Perovskite solar cells (PSCs) hold great promise for space photovoltaics (PV) due to their impressive PV performance, excellent power-to-weight ratio, and cost-effectiveness. However, the environment in space presents numerous challenges for solar cells, especially cosmic radiation. PSCs have shown remarkable resistance to various forms of radiation, such as electrons, protons, ultraviolet, and γ-rays. Nevertheless, their stability in space applications still lags behind that of crystalline silicon (c-Si) and gallium arsenide (GaAs) cells. To facilitate the application of PSCs in space, it is vital to enhance their long-term stability. This mini-review examines the radiation resistance of PSCs, explores the mechanisms behind radiation-induced damage, and proposes potential strategies to bolster their resistance to radiation and reinforce overall stability.

Received 20th October 2023
Accepted 14th December 2023

DOI: 10.1039/d3ta06388g

rsc.li/materials-a

1. Introduction

Metal halide perovskites (MHPs) are semiconductor materials known for their exceptional properties, allowing them to be widely utilized across various industries. These materials typically exhibit direct-transition semiconductor behavior, characterized by a high absorption coefficient and a low exciton binding energy, resulting in excellent PV performance. Furthermore, MHPs display efficient carrier transport rates, long carrier lifetimes, and significant diffusion lengths, enabling effective transfer of electrons and holes with minimal recombination.[1] Perovskite solar cells (PSCs) utilizing MHPs as the absorbing layer have emerged as examples of third-generation solar cells. A significant milestone in the development of PSCs was achieved in 2009 when Miyasaka *et al.* replaced the absorbing material in dye-sensitized solar cells with perovskite, resulting in a photovoltaic conversion efficiency (PCE) of 3.8%.[2] Since then, PSCs have garnered significant attention, and their PCE has experienced rapid growth, as depicted in Fig. 1(A).[3–9] Currently, single-junction PSCs have achieved a certified PCE of 26.14%,[10] steadily approaching the Shockley–Queisser efficiency limit of 33.7%.[11]

The high light absorption coefficient of MHPs allows for a significant reduction in the thickness of the absorption film to just a few hundred nanometers, providing PSCs with a high power-to-weight ratio (Fig. 1(B)). In comparison, traditional c-Si cells possess a ratio of less than 1 W g^{-1} due to their thicker light-absorbing layer.[12] Triple-junction III–V semiconductor cells achieve a ratio of roughly 3 W g^{-1} through their densely fabricated structure. In contrast, flexible single-junction PSCs can reach an impressive ratio of 23–29 W g^{-1}, while multi-junction PSCs can surpass even that, reaching an outstanding ratio of 79–83 W g^{-1}.[13,14] Based on the above comparison, the PSCs are undoubtedly better suited to meet the needs of spacecraft for lightweight energy systems. However, the long-term stability of PSCs remains the main obstacle to their pragmatic applications. Moisture can lead to hydrolysis in MHPs, while oxygen molecules can interact with photogenerated electrons in the conduction band, resulting in the formation of superoxide (O_2^-) and accelerating the decomposition of MHPs.[15] If PSCs can be utilized in a space environment devoid of moisture and oxygen, these two prominent factors will be negligible, making PSCs very promising for space deployment.

While plenty of current studies on PSCs have been conducted for ground applications, there is a lack of studies focusing on their suitability in space. The space environment poses challenges due to its complexity and variability, subjecting PSCs to harsh conditions such as extreme radiation, ultra-high vacuum, and severe temperature fluctuations.[16] Moreover, the exorbitant cost of space flight makes it practically impossible to repair or replace PSCs once they are deployed in space. Therefore, PSCs must exhibit long-term stability and reliability to ensure the safety of spacecraft. Fortunately, research has

[a]Shanghai Institute of Optics and Fine Mechanics, Chinese Academy of Sciences, 201800, Shanghai, China. E-mail: yifanzheng@siom.ac.cn; shaoyuchuan@siom.ac.cn
[b]Center of Materials Science and Optoelectronics Engineering, University of Chinese Academy of Sciences, 100049, Beijing, China
[c]Beijing Institute of Spacecraft Environment Engineering, Beijing 100094, China
[d]Science and Technology on Power Sources Laboratory, Tianjin Institute of Power Sources, Tianjin, 300384, China

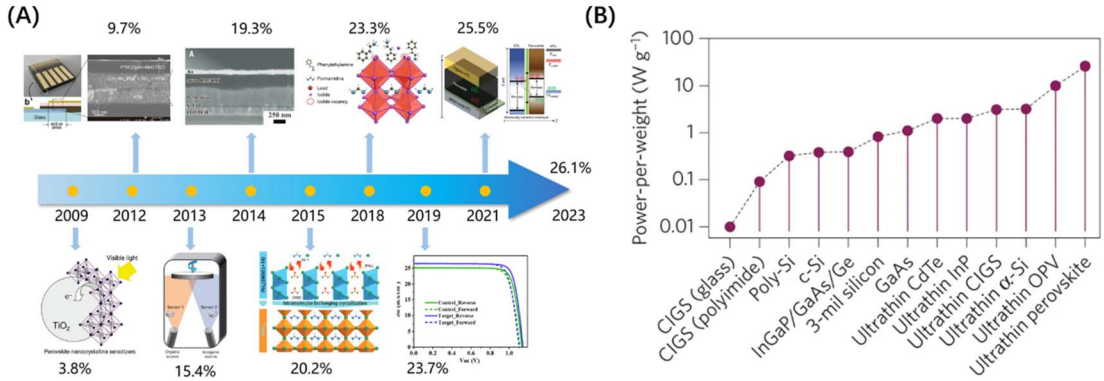

Fig. 1 (A) Schematic of the rapid development of PCE for PSCs. (B) Comparison of the power-to-weight ratio of common solar cells.[14] Copyright 2015, Springer Nature.

shown promising results regarding the strong radiation resistance of PSCs.[12,13,17,18] Compared with c-Si cells and III–V cells, PSCs can withstand radiations such as electron radiation and proton radiation with higher energy and flux, making them excellent candidates for space PV. To fully realize the potential of PSCs for space applications, further research is needed to understand the mechanisms underlying radiation damage and resistance, enhancing the stability of PSCs.

This paper aims to provide a comprehensive overview of the radiation resistance of PSCs and their potential applications in the space environment. Firstly, we will describe the characteristics of the space environment and their effects on PSCs. Next, we will delve into the resistance of PSCs against electron radiation, proton radiation, γ-ray radiation, and ultraviolet (UV) irradiation, while examining the underlying mechanisms of radiation damage. In addition, we will propose reinforcement methods that can mitigate ionization damage and displacement damage caused by radiation in PSCs. Finally, we will conclude with a summary and provide an outlook for future research in this field.

2. Influences of the space environment on PSCs

2.1 Characteristics of the space environment

The space environment is an intricate system that can be difficult to describe accurately. To provide a comprehensive understanding, NASA's Marshall Space Flight Center (MSFC) has identified seven key elements that characterize the space environment. These elements include plasma, geomagnetic field, cosmic rays, neutral atmosphere, space debris, thermal fluctuations, and solar activity.[17]

To provide a brief categorization of the seven factors mentioned above, we can first consider their micro-level effects. The space particle radiation environment can be classified into Van Allen radiation belts, solar cosmic rays (SCRs), and galactic cosmic rays (GCRs), as shown in Fig. 2(A).[19] The geomagnetic field can trap charged particles to create the inner and outer Van Allen radiation belts.[20–22] The inner belts, located 100–10 000 km above the surface, mainly consist of protons and electrons, with small amounts of heavy ions. On the other hand, the outer belts, positioned at an altitude of approximately 13 000–60 000 km, predominantly contain high-energy electrons (0.1–10 MeV) along with a limited number of protons. The fluxes of these two types of radiation in space near the Earth are shown in Fig. 2(B). The Sun has the most significant impact on Earth among astronomical objects, and the particle density in the SCRs is usually several orders of magnitude higher than GCRs.[23] The Sun's upper atmosphere continuously emits a stream of supersonic charged particles such as electrons, protons, helium nuclei, and small amounts of heavy ions.[19] These streams of particles are hot enough to form plasma and travel close to Earth's orbit at speeds of 300 to 900 km s^{-1}. GCRs are streams of high-energy charged particles from outside the solar system that reach Earth at nearly the speed of light, including protons and electrons as the most dominant constituents, as well as ultraviolet light, γ-rays, X-rays, and other constituents.[24]

Then we consider the macro-level effects including neutral atmosphere, space debris, and thermal fluctuations.[25] The effects of the neutral atmosphere on spacecraft primarily involve atomic oxygen and an ultrahigh vacuum environment.[26–28] Space debris refers to meteoroids and space junk orbiting the Earth at speeds close to the first cosmic velocity of 7.9 km s^{-1}, which can wear out or even disintegrate spacecraft by collision.[29,30] Thermal fluctuations are mainly caused by the absence of heat conduction and convection in a vacuum environment.[18] Direct solar radiation can cause spacecraft to reach temperatures exceeding 100 °C, whereas entering the Earth's shadow zone can lead to temperatures dropping below −100 °C.[25] This temperature variation is further compounded by the rapid nature of low-orbiting spacecraft, which complete an orbit around the Earth in approximately 90–100 minutes, subjecting them to dramatic and rapid temperature cycling.

2.2 Influences and requirements of the space environment

Although PSCs offer advantages for space applications, it is important to acknowledge the impact of various factors in the space environment on them, as depicted in Fig. 3. Certain engineering programs can shield some of the seven factors mentioned above.[31–33] Nevertheless, radiation, thermal

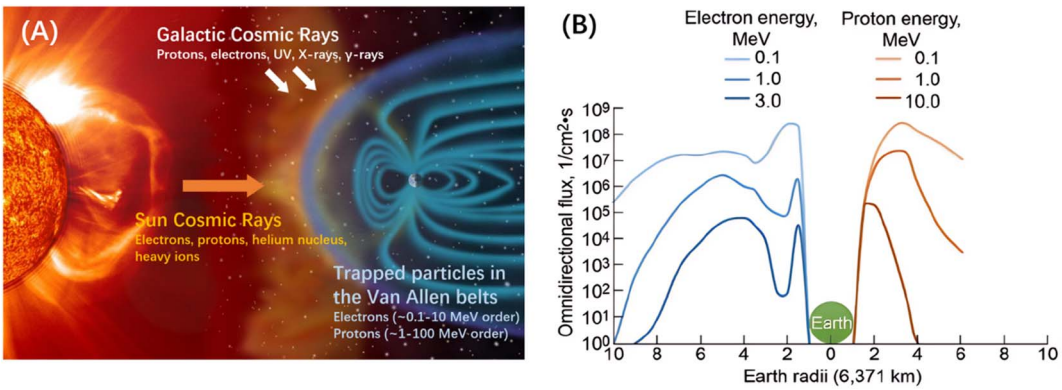

Fig. 2 (A) Schematic view of the Van Allen belts, SCRs, and GCRs. Copyright 2002, NASA. (B) Flux of electron and proton radiation around the Earth.[17] Copyright 2022, American Chemical Society.

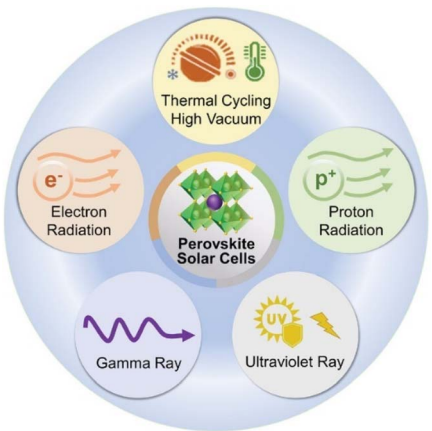

Fig. 3 The main factors affecting PSCs in the space environment.[12] Copyright 2021, Wiley.

fluctuations, and ultrahigh vacuum can still pose significant challenges to PSCs. In the follow-up discussion, we will focus on radiation-induced damage and will not specifically address temperature and vacuum.

Radiation-induced damage can be classified into two types: ionization damage and displacement damage.[20] Ionization damage occurs when incident particles interact with MHPs, leading to the ionization of target atoms. This process generates additional hole–electron pairs, triggering various effects such as single-particle event effect (SEE), total ionizing dose effect (TID), surface charge–discharge effect, and internal charge effect.[24,34] Additionally, ionization damage can also result from high-energy photons breaking chemical bonds and leading to the formation of new bonds, causing changes in the physical and chemical properties of MHPs. Displacement damage is predominantly caused by cumulative effects from non-ionizing radiation, including protons, heavy ions with various energy levels, and electrons with energies exceeding 150 keV.[35] When incident particles interact with atoms, they transfer kinetic energy and cause the atoms to shift from their original positions, resulting in the creation of vacancies. These vacancies, along with interstitial atoms, serve as active recombination centers. The formation of a defect structure due to displacement damage further contributes to carrier scattering and diminishes carrier mobility.

The demanding conditions of the space environment necessitate specific requirements for PSCs, which can be succinctly summarized as long-term stability, high performance, and high power-to-weight ratio. Firstly, ensuring long-term stability is the most important issue, since the spacecraft power systems must exhibit absolute stability and reliability. Commonly used c-Si cells have a service life exceeding 20 years, which is in line with the typical field warranty for PV panels.[36] Currently reported lifetimes of PSCs are less than five years,[37–39] mainly affected by moisture, oxygen, and degradation caused by illumination, bias, and temperature, but have the potential to be enhanced to more than 25 years.[40] The absence of moisture and oxygen in space provides great advantages for enhancing the long-term stability of PSCs, deserving more research to realize this potential. Secondly, achieving high performance is crucial for PSCs as they serve as the primary energy source. Although current single-junction PSCs have achieved an impressive PCE of 26.14% on the ground, getting closer to single-crystalline Si cells (26.8%) and GaAs cells (27.8%),[10] radiation and thermal fluctuations will inevitably degrade materials and lead to a decline in PCE. Further research is necessary to maintain high PCE in space. Lastly, the power-to-weight ratio is necessary as it represents the electric power that can be provided per unit weight. Flexible PSCs have shown superior power-to-weight ratios compared to c-Si and III–V cells. Developing support structures and application methods for flexible PSCs in aerospace engineering could lead to cost savings in space development projects.

3. Radiation resistance and damage mechanisms of PSCs

3.1 Electron radiation

Electrons play a prominent role as energetic particles in the space environment, influencing the dielectric properties of photosensitive materials.[12] Specifically, electron radiation can induce both ionization damage and displacement damage in MHPs.

To explore this further, we examined studies that have investigated the resistance of MHPs to electron radiation. Commonly used cells like c-Si cells, GaAs cells, and InGaP/GaAs cells in spacecraft suffered severe damage when exposed to electron-beam (EB) irradiation. The maximum power (P_{max}) of the c-Si cells decreases to 80% of the pre-irradiation level when the EB (1 MeV) radiation dose reaches 10^{15} e per cm^2 and further decreases to 60% when the radiation dose comes to 10^{16} e per cm^2.[41] The III–V cells are in the same situation, with 84% P_{max} retained under the 10^{15} e per cm^2 EB (1 MeV) dose and 75% under the 10^{16} e per cm^2 dose.[42,43] In 2015, Hirose *et al.* conducted the first study on PSCs under electron radiation. They exposed $MAPbICl_2$ PSCs to an EB with 1 MeV energy and a dose of 10^{16} e per cm^2, irradiating them from the metal electrode side. More than 93% of photovoltaic performance was retained including short-circuit current density (J_{SC}), open-circuit voltage (V_{OC}), and maximum power (P_{max}).[43] It became evident that PSCs exhibited superior resistance to electron radiation. Then in 2018, Miyasaka *et al.* also investigated the performance of PSCs under high flux EB irradiation.[44] PSCs with $MAPbI_3$ as the light-absorbing layer, and P3HT and TiO_2 as the carrier transporting layers (CTLs) managed to retain over 90% of the original EQE, as shown in Fig. 4(A) and (B). This study further highlights the remarkable tolerance of PSCs to EB irradiation. In the studies mentioned above, the control devices have relatively low PCE. In 2019, Yan *et al.* investigated the electron radiation resistance of PSCs with a PCE exceeding 20%, as shown in Fig. 4(D).[45] When the radiation dose reached 1.3×10^{15} e per cm^2, the V_{OC} and fill factor (FF) could still maintain approximately 90% of their unirradiated levels. However, J_{SC} decreased to around 70% of its unirradiated level, and the PCE dropped to less than 60% of its unirradiated level (Fig. 4(C)). This decline can be attributed to the darkening of the glass substrate and the degradation of MHPs. As shown in Fig. 4(E), the darkening glass substrate has a significant effect on optical transmittance, which can be reduced to less than 40%. The authors suggest that replacing the glass with a more appropriate substrate will enhance the potential of PSCs for space applications.

It's vital to understand how electron radiation impacts PSCs if we want to utilize and further enhance electron resistance. In this case, Xiao *et al.* used cathodoluminescence (CL) spectroscopy to examine the radiation damage on $MAPbI_3$ thin films caused by EB.[46] They proposed two mechanisms to explain the damage: the generation of defects due to collisions and structural phase transition caused by the heating effect of the EB. They normalized the CL data of $MAPbI_3$ thin films and observed no significant change in the signal intensity during the initial period under an accelerating voltage of 2 kV. The full width at half maximum (FWHM) slightly increased after 3 minutes. When the voltage was raised to 10 kV, as shown in Fig. 5(A), there was a notable decrease in the CL peak with increasing current. Additionally, the CL peak showed a blue shift with increasing time. They attributed the decrease and broadening of the CL peak to defects induced by the EB. Energetic electrons displaced atoms within the perovskite lattice, resulting in Frenkel defects. These defects introduced non-radiative recombination centers, leading to a reduction in the CL peak of the exciton after electron irradiation. The lattice structure distortion caused by the defects also contributed to the broadening of the CL peak. Regarding the blue shift observed in the CL peak, the authors demonstrated through low-

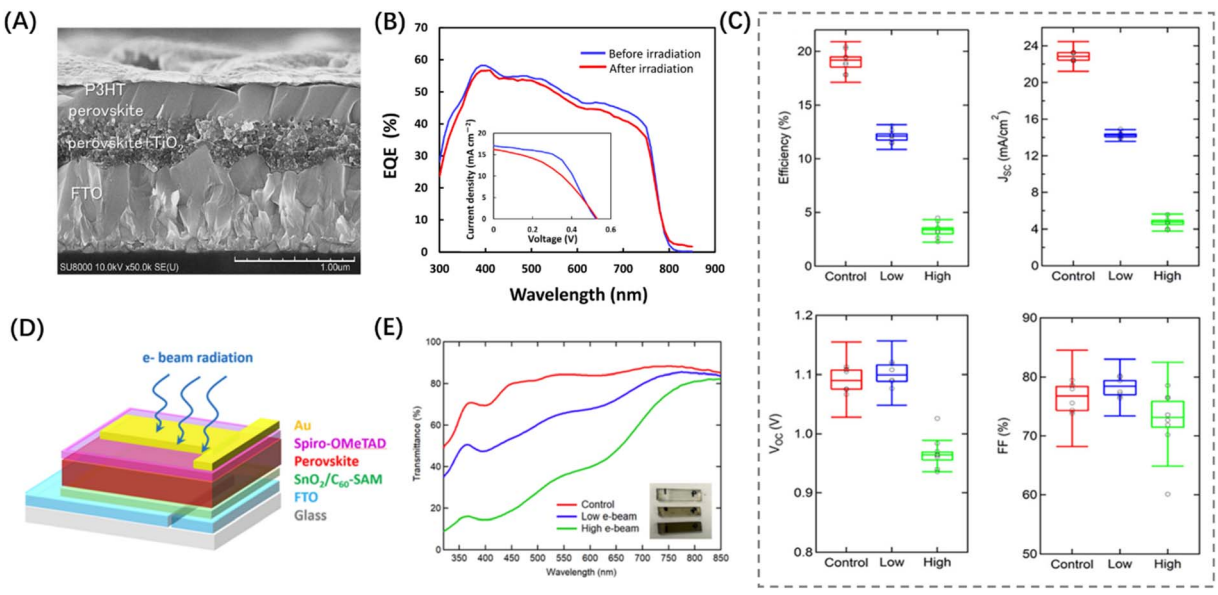

Fig. 4 (A) Cross-sectional SEM image of the P3HT-$MAPbI_3$ PSCs employed for electron radiation tolerance measurements. (B) EQE and *J*–*V* performance (insertion) of the P3HT-$MAPbI_3$ PSCs recorded before and after the 1 MeV EB irradiation with a dose of 10^{16} p per cm^2.[44] Copyright 2018, Elsevier. (C) Distributions of PV parameters for PSCs under control and low and high EB irradiation. (D) Schematic of a PSC used for the electron radiation test. (E) Optical transmittance of FTO glass substrates before and after EB irradiation.[45] Copyright 2020, American Chemical Society.

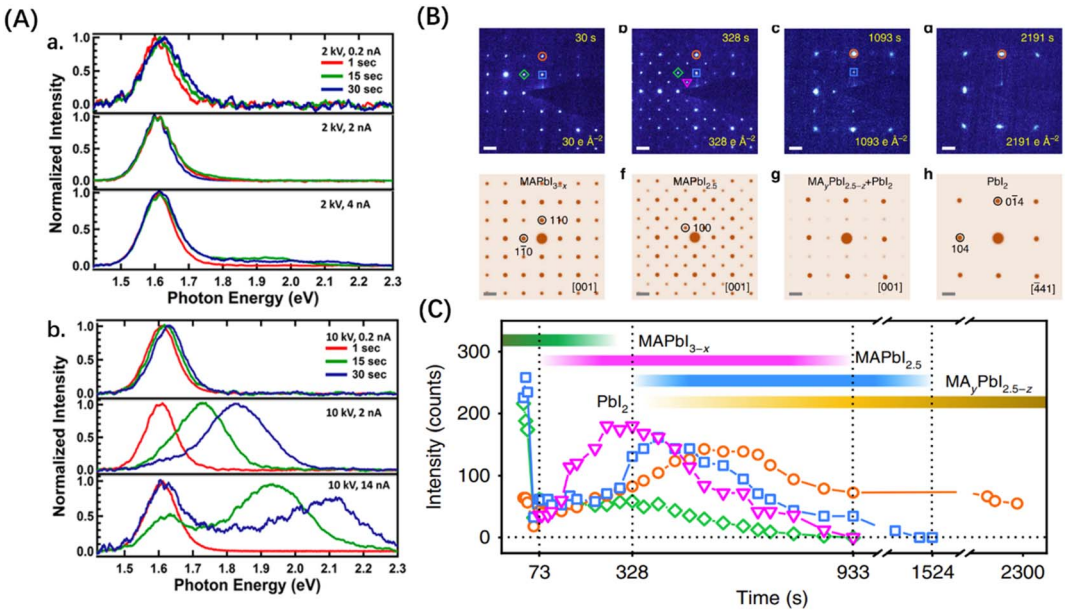

Fig. 5 (A) Normalized CL spectra as a function of beam voltage, beam current, and irradiation time.[46] Copyright 2015, American Chemical Society. (B) Time-series SAED patterns and corresponding simulated ED patterns showing that the structure decomposes from $MAPbI_3$ to PbI_2. (C) Variation of diffraction intensities of various components with time during the decomposition of $MAPbI_3$.[47] Copyright 2018, Springer Nature.

temperature experiments that it resulted from the decomposition of the perovskite due to the heating effect of the EB. This decomposition generated unstable intermediate phases at levels higher than the bandgap, causing a rapid change in the CL peak value and width within 30 seconds.

Material composition analyses can be used to dynamically observe the process of degradation of MHPs. Chen *et al.* used electron diffraction (ED) patterns and selected area electron diffraction (SAED) to observe the decomposition of $MAPbI_3$ under EB irradiation and plotted the diffraction intensity as a function of time, as shown in Fig. 5(B) and (C).[47] Initially, desorption occurs, leading to the ionization of I^- and the formation of the superstructure $MAPbI_{2.5}$. Subsequently, both MA^+ and I^- are lost simultaneously, resulting in the formation of $MA_yPbI_{2.5-z}$ ($0 \leq y \leq 1$, $0 \leq z \leq 0.5$). Eventually, the superstructure undergoes decomposition, transforming into hexagonal PbI_2. The breaking of C–N bonds in MA^+ results in the formation of NH_3 and HI, leading to the generation of polymeric hydrocarbon residues ($-CH_2-$) on the surface.[48] Dang *et al.* conducted a study on the impact of EB irradiation on inorganic perovskites, specifically $CsPbI_3$ and $CsPbBr_3$. Similar to $MAPbI_3$, desorption causes the detachment of halogen ions, conversion of Pb^{2+} ions to Pb^0 atoms, and decomposition of the perovskite.[49]

This section has demonstrated the enhanced electron radiation resistance of PSCs in comparison to conventional PV. EB irradiation can lead to the darkening of the glass substrate, the formation of non-radiative recombination centers, and the accelerated decomposition of MHPs. To address these detrimental effects, targeted approaches can be employed to further enhance the resistance of MHPs to electron radiation.

3.2 Proton radiation

Protons are 1800 times heavier than electrons. When they interact with perovskite, the primary energy loss occurs through ionization, resulting from inelastic collisions with extra-nuclear electrons. When protons collide with the atomic nucleus, their state undergoes minimal change, leading to relatively low energy loss. Despite this, the impact of the proton on the target atom should not be ignored, as it can yield substantial displacement damage.

It has been demonstrated that PV materials commonly utilized in space, such as c-Si, GaAs, and InP, are more susceptible to proton radiation compared with MHPs.[50,51] Proton radiation tests on PSCs primarily involve irradiating the unprotected backside with low-energy protons ranging from 50 to 150 keV, or irradiating the front of the device with high-energy protons ranging from 20 to 68 MeV to observe factors compared to the pre-irradiation period.[13] The selection of these energy values aims to represent the spatial distribution of proton energies. Higher energy protons are infrequently encountered in space, with acceleration to GeV level energies occurring only in special events like massive solar flare eruptions.[52] Lang *et al.* subjected the $MAPbI_3$ cells to proton radiation with an energy of 68 MeV and a dose of 1.02×10^{13} p per cm^2.[53] The experimental findings shown in Fig. 6(A) reveal that the V_{OC} and FF of the device remain relatively unchanged. However, the J_{SC} experiences a decrease of approximately 40% at 1.02×10^{13} p per cm^2, compared to only about a 10% decrease at 1×10^{12} p per cm^2. When testing c-Si cells under the same conditions, the J_{SC} decreased by 40% at a fluence of just 7×10^{11} p per cm^2, indicating that $MAPbI_3$ is more resistant to proton radiation than c-Si. Furthermore, it is worth mentioning

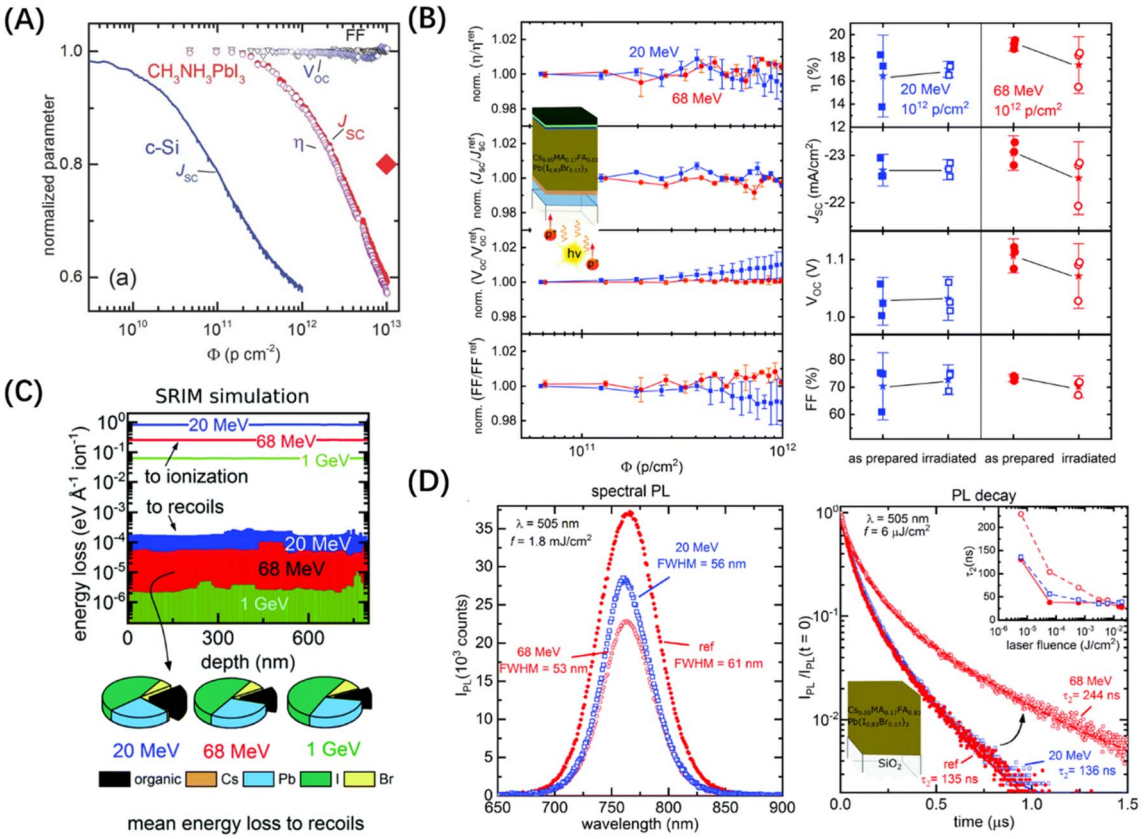

Fig. 6 (A) Normalized solar-cell parameters as a function of the proton dose.[53] Copyright 2016, Wiley. (B) Evolution of η, J_{SC}, V_{OC}, and FF of a set of $Cs_{0.05}MA_{0.17}FA_{0.83}Pb(I_{0.83}Br_{0.17})_3$ based solar cells during 20 and 68 MeV proton irradiation as a function of the accumulated proton dose and statistics taken prior to and after a proton irradiation dose of 10^{12} p per cm^2. (C) Energy loss of 20 MeV, 68 MeV, and 1 GeV protons to ionization and recoils within the $Cs_{0.05}MA_{0.17}FA_{0.83}Pb(I_{0.83}Br_{0.17})_3$ absorber as a function of the layer depth by SRIM simulation. (D) PL spectra and normalized TRPL of reference and proton irradiated perovskite thin-films on quartz.[54] Copyright 2019, Royal Society of Chemistry.

that the J_{SC} of the $MAPbI_3$ cells undergoes self-healing after the cessation of proton radiation. Lang *et al.* also demonstrated that $Cs_{0.05}MA_{0.17}FA_{0.83}Pb(I_{0.83}Br_{0.17})_3$ cells exhibit excellent resistance to high-energy, high-throughput proton radiation.[54] As shown in Fig. 6(B), the device exhibited a PCE of 18.8% under AM0 illumination before radiation. Following exposure to proton radiation with an energy of 68 MeV and a dose of 1×10^{12} p per cm^2, which is about the accumulated proton radiation dose for a three-year operation in space, it retained approximately 95% of its initial PCE.

Regarding the mechanism behind proton radiation-induced defects in MHPs, Lang *et al.* found that a 1 mm thick quartz substrate could effectively shield against proton radiation below 10 MeV. However, protons with energies of 20 MeV, 68 MeV, and 1 GeV were able to penetrate the substrate with minimal attenuation and reach the perovskite layer. Subsequently, they undergo collisions and release energy. Through these inelastic collisions, the energy of the protons is transferred to the atoms, exceeding the displacement threshold, especially for hydrogen atoms. This leads to the creation of vacancies and the formation of recombination centers.[54] The mechanism described above is supported by other studies. For instance, in organic solar cells, the extraction of H from C–H bonds is identified as the primary process leading to radiation-induced defect formation.[55] Additionally, it has been observed that photon irradiation exceeding 2.7 eV can cause the rupture of N–H bonds in $MAPbI_3$.[56,57] In the SRIM simulations conducted by Lang's study, it was found that 20 MeV protons will stay in the perovskite layer due to their weaker penetration capability compared to 68 MeV protons. As a result, the energy decay of the former is an order of magnitude higher, as shown in Fig. 6(C), causing more C–H and N–H bond breakage and H atom displacement. However, *J–V* curves, photoluminescence (PL) spectroscopy, and time-resolved photoluminescence (TRPL) spectroscopy revealed that the impact of 20 MeV protons was small, while 68 MeV protons had a significant influence on device performance and the mechanism of carrier recombination, as shown in Fig. 6(D). Lang *et al.* concluded that the detachment of H atoms from chemical bonds does not lead to localized defects. Instead, they observed that these H atoms rapidly migrate back into the cations, enabling the organic cations to undergo a self-healing process. Similar self-healing phenomena in $MAPbI_3$ have also been explored by several groups. Additionally, low-temperature experiments have provided evidence of the sub-stability of H defects, further supporting the existence of such self-healing mechanisms.[57,58]

Lang *et al.* also explained the damage mechanism caused by 68 MeV proton radiation.[54] They proposed that a higher amount of energy is absorbed by the inorganic components, resulting in the displacement of a greater number of I or Pb atoms that do not return to their original lattice positions. This process particularly leads to the formation of defects related to iodine. First-principles calculations have confirmed that iodine-related defects in perovskite serve as highly active recombination centers.[59] Consequently, controlling the presence of iodine-related defects, such as by introducing additional iodine ions, can further enhance the resistance of PSCs to proton radiation.[60]

In this section, we have discussed the proton radiation resistance of PSCs and the self-healing ability of MHPs in response to the displacement of H atoms caused by proton radiation. However, the displacement of Pb and I atoms by high-energy protons can result in the formation of defects with significant implications. Given the high energy levels of protons, it is crucial to prioritize material enhancements when designing shielding strategies. By adopting comprehensive approaches, we can effectively enhance the proton resistance of PSCs from various perspectives.

3.3 Gamma-ray radiation

In the previous section, we discussed direct ionizing radiation, which can directly damage the macromolecular structure and impact the performance of PSCs. However, it is equally important to consider the impact of indirect ionizing radiation, such as γ-rays and neutron radiation. In terms of γ-rays, photons lack rest mass and charge, resulting in the absence of collisions and coulombic interactions with atoms. Nevertheless, γ-rays can interact with perovskite through the photoelectric effect and Compton effect, generating secondary particles that indirectly ionize other atoms. Over a 20 years operation in space, a solar cell can accumulate a dose of approximately 1000 kRad of γ-ray radiation.[17]

Boldyreva *et al.* conducted a study on the effects of γ-ray radiation on commonly used MHPs.[61] They exposed perovskite films to γ-rays at doses ranging from 10 to 500 kRad and analyzed their X-rays diffraction (XRD), X-rays photoelectron spectroscopy (XPS), optical UV-vis spectroscopy, and PL measurements. Comparing the XPS energy spectra before and after radiation, it was observed in Fig. 7(A) that the Pb 4f-spectra of $MAPbI_3$ shifted towards PbI_2, indicating the loss of the MAI and the formation of PbI_2 on the surface, and the Pb 4f-spectra of $CsPbI_3$ suggested the formation of Pb^0. Since $CsPbI_3$ does not release organic volatile products from the organic component such as MAI, it further degraded into Pb^0 and I_2 gas. The UV-visible spectra exhibited only minor differences among the samples. The authors exposed the substrate glass to γ-rays and discovered a significant decrease in the transparency, particularly in the 300–600 nm range. This decrease is attributed to ionization-generated carriers being bound in vacancies or impurities, forming color centers.[62] After accounting for the darkening effect of the glass, it was observed that $MAPbI_3$ exhibited the highest stability under γ-rays compared to the other samples. Even after exposure to a dose of 1000 kRad γ-rays, the experimental values remained consistent with the calculated values, as depicted in Fig. 7(A). This suggests that the decay in the performance of $MAPbI_3$ can be attributed to factors other than the darkening effect of the glass. The authors interpreted the phenomenon as a self-healing mechanism, involving the reversible generation of $MAPbI_3$, the passivation effect of iodine vacancies, and the promotion of chemical reactions induced by γ-rays, as shown in Fig. 7(B).

There are also many studies describing the γ-ray resistance of PSCs.[63–65] The higher atomic number of Pb, which offers greater radiation resistance, along with the self-healing properties of MHPs, gives PSCs an inherent advantage in terms of radiation resistance. Considering the substantial penetration of γ-rays, it is essential to prioritize material optimization to enhance resistance without adding unnecessary weight to space launches.

3.4 UV radiation

The atmosphere surrounding the Earth can scatter and absorb sunlight, resulting in a completely different solar spectrum on the ground than outside the atmosphere. The spectrum of sunlight as it reaches the upper interface of the atmosphere is defined as air mass zero (AM0), and the standard spectrum of the ground is noted as AM1.5G, where 1.5 represents the cosine of the solar zenith angle. As shown in Fig. 8(A), compared to the standard AM1.5G spectra, AM0 spectra exhibit a higher concentration of UV irradiation.[13] Studies have shown that UV is one of the main factors affecting the stability of PSCs.[66] Inside the atmosphere, the performance of PSCs decreases under the influence of UVA (320–400 nm) and UVB (280–320 nm).[67] The UV resistance of PSCs in ground-based studies has been greatly improved. Outside the atmosphere, the existence of UVC (200–280 nm) and UVD (100–200 nm) with higher energy requires further study to enhance the UV hardness of PSCs in space.

UV radiation possesses high frequency and short wavelength, inducing the breakage of chemical bonds within the polymer material. Prolonged exposure to UV radiation generates abundant polar radicals, leading to the formation of new molecules after recombination and the degradation of the material.[35] Firstly, we can enhance the stability by increasing the UV hardness of perovskite materials. Ouafi *et al.* found higher UV stability of $MAPbBr_3$ than $MAPbI_3$ resulting from the cubic form which is more stable and denser.[68] When the bromide fraction achieves 20% or more in $MAPb(I_{1-x}Br_x)_3$, the UV stability of the unencapsulated perovskite is improved markedly, as shown in Fig. 8(C). Wang *et al.* utilized sunscreen perovskite using the tautomeric molecule 2-hydroxy-4-methoxybenzophenone to restrain the degradation caused by UV tautomeric transition and enhance the passivation by improving the defect formation energy to −1.35 eV for the stable coordination.[67] This work prominently passivated the defect and prevented the perovskite film from degrading, improving the PCE to 23.09% and the stability under UV simultaneously.

UV radiation can also cause degradation through the photocatalysis of metal oxides. For instance, TiO_2 has a large number of oxygen vacancies that allow for oxygen absorption and release, generating deep energy level defects that lead to recombination and catalytic degradation.[18] Li *et al.* indicated that TiO_2 also undergoes UV degradation in an inert gas atmosphere. They

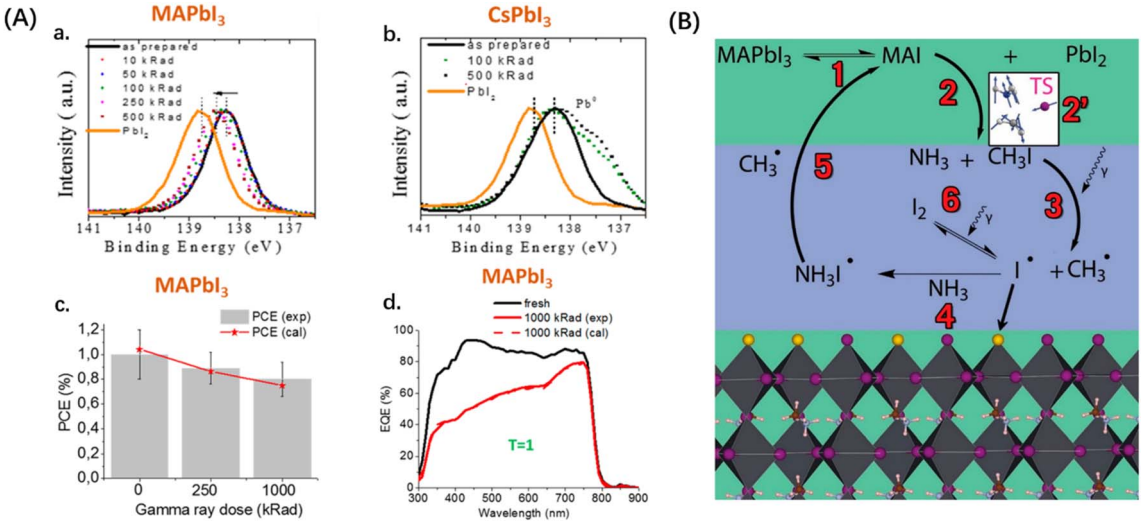

Fig. 7 (A) (a and b) Evolution of XPS Pb 4f of thin $MAPbI_3$ and $CsPbI_3$ films under gamma ray exposure (10–500 kRad); (c) evolution of the solar cell PCE under gamma-ray exposure. Red lines show the expected behavior in case gamma rays induce only substrate darkening without damaging the PV stack itself. (d) Evolution of EQE spectra of the devices after 1000 kRad gamma ray exposure. EQE spectra were modeled according to glass transmittance. The T-factor is the ratio of the experimentally obtained J_{SC} and calculated J_{SC}. (B) Diagram showing mechanisms of $MAPbI_3$ decomposition based on theoretical calculations. A green background indicates a solid state while a blue background indicates the gas phase.[61] Copyright 2020, American Chemical Society.

proposed a two-stage degradation of TiO_2-based PSCs, as shown in Fig. 8(B),[69] where UV radiation generates additional holes in the valence band of TiO_2, transforming Ti^{3+} defects into Ti^{4+} defects that generate non-radiative recombination centers. With the increase in Ti^{4+} concentration, I^- ions in perovskites are oxidized to I_2 or rather I_3^-, promoting the decomposition of perovskites into PbI_2 as well as HI gas, causing the performance and stability of PSCs to deteriorate. To avoid this phenomenon, photocatalytically inactive films are required to reduce UV-induced degradation. SnO_2 is an excellent choice for this requirement, which can also provide high electron mobility and fast electron extraction.[70–74] We can also take measures to shield or inhibit the

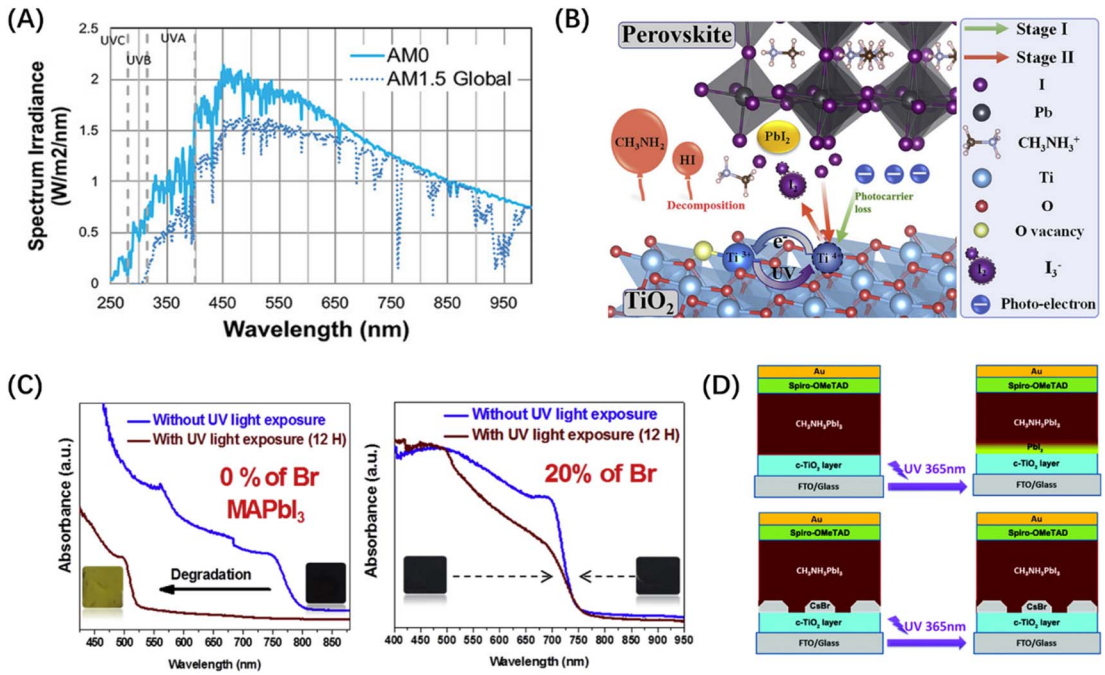

Fig. 8 (A) Space (AM0) and Earth (AM1.5G) solar spectrum.[13] Copyright 2021, Wiley. (B) The mechanism of PSC degradation under continuous UV irradiation.[69] Copyright 2020, Elsevier. (C) UV-vis absorption spectra of $MAPb(I_{1-x}Br_x)_3$ films with different bromide fractions (0 and 20%) before and after 12 h of exposure to UV irradiation.[68] Copyright 2018, Elsevier. (D) Schematic illustration of the control PSCs before and after UV irradiation, and PSCs with CsBr interface modification before and after UV irradiation.[77] Copyright 2016, Royal Society of Chemistry.

photocatalysis of TiO_2. Some researchers used Al_2O_3 as a scaffold to support perovskites and sensitized films, protecting them from degradation by moisture and UV.[75,76] Snaith *et al.* used CsBr for modification at the TiO_2/perovskite interface of the p-i-n PSCs to enhance UV hardness.[77] They confirmed that CsBr was not incorporated into the perovskite lattice, but acted as an independent interface modification layer to inhibit the photocatalytic ability of TiO_2, as shown in Fig. 8(D). Meanwhile, this method improves the energy band structure of PSCs and boosts the efficiency of carrier transport at the TiO_2/perovskite interface.

This section has summarized how UV affects PSCs and some measures to enhance UV hardness. We can take both internal and external approaches to minimize the degradation caused by high-energy photons. Internally, we can enhance the UV hardness of perovskites themselves by improving the lattice structure and passivating internal defects, while externally we can replace the substrate or modify the interface to inhibit the active photocatalytic effect caused by metal oxide.

4. Reinforcement of PSCs for space application

4.1 Ionizing damage

Ionization can have a significant impact on PSCs, primarily by causing coloration of the glass substrate. This can affect the device's transmittance and lead to a substantial decrease in J_{SC} and PCE. This phenomenon is commonly observed in both electron and γ-ray resistance experiments.[45,61,78] Incident radiation separates extra-nuclear electrons from the atoms, generating additional hole–electron pairs.[79] Some of these free electrons and the resulting holes can be trapped in defects, such as ionic vacancies, impurities, and unbridged oxygen atoms, absorbing light by energy level transition with the exact frequency. These optically active defects are known as color centers.[62] To maximize the suitability of PSCs for space applications, it is essential to identify substrates that can resist darkening when exposed to radiation.

Ionization can also affect MPHs, not only through extra carriers but by disrupting chemical bonds. In addition to choosing materials with high radiation hardness, we can also take reasonable encapsulation measures. For example, when PSCs are exposed to UV radiation, the extra holes can enhance the photocatalytic ability of metal oxides acting as CTLs and accelerate the decomposition of MHPs. To effectively mitigate the impacts of UV radiation, a commonly employed strategy is converting high-energy UV into low-energy photons. Bella *et al.* presented a fluorescence process by V570-doped UV coatings, which absorbs the energy of UV radiation and re-emits it in the visible light range, as shown in Fig. 9(A) and (B).[80] This approach not only avoids the instability caused by UV radiation but significantly increases the J_{SC} of the PSCs and improves the PCE (Fig. 9(C)). The J_{SC} improvement is attributed to a significant increase in IPCE in the UV range (Fig. 9(D)). The target devices with UV coatings maintained good PCE stability under UV irradiation (5 mW cm^{-2}) for over 6 months.

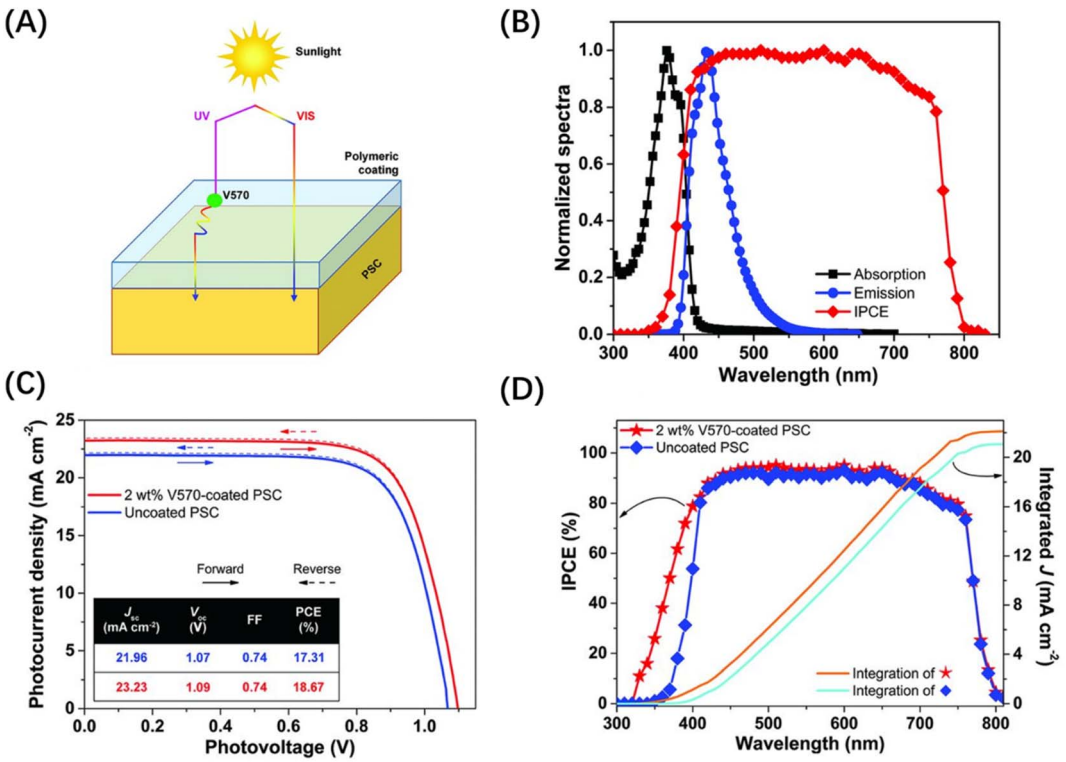

Fig. 9 (A) Scheme of the V570-doped UV coating operating principle. (B) Normalized absorption and emission spectra of V570-doped UV coating compared with the IPCE response of the PSCs. (C and D) Photovoltaic characterization including *J*–*V* and IPCE curves of the best device.[80] Copyright 2016, The American Association for the Advancement of Science.

Ionization also presents various space engineering challenges that require careful consideration. The SEE and TID can be mitigated by protecting and detecting electrical circuits. Circuit malfunctions can arise from electromagnetic pulses resulting from surface charging and discharging effects.[24] To address these concerns, it is advisable to employ conductive coatings or select surface materials with low resistivity and a high secondary electron emission rate. Additionally, equipping the spacecraft with surface potential detectors and active control equipment allows for in-orbit monitoring and control of surface charging and discharging effects. To minimize the risks associated with internal charging effects, shielding and grounding techniques can be implemented.[81]

4.2 Displacement damage

To alleviate the effects of displacement damage on PSCs, a promising approach is to prioritize the selection and development of resilient materials. One effective method is to enhance the energy threshold for atomic displacement by increasing the bonding energy of halogen atoms and improving the phase stability of perovskites. For example, Liu *et al.* successfully stabilized $CsPbCl_3$ nanocrystals by modifying the perovskite precursors with Mn^{2+} doping, resulting in a 10-fold increase in lifetime under 200 keV electron radiation.[82] This approach effectively increased the electron radiation resistance of perovskite nanocrystals. Using first-principles calculations, they found that $CsPb_{1-x}Mn_xCl_3$ is more stable than $CsPbCl_3$ due to the stronger Mn–Cl and Pb–Cl bonds, which reduce the desorption of Cl^-. The formation energy ΔH of Mn^{2+} replacing Pb^{2+} is also less than zero, indicating that the material becomes more stable. The $CsPbCl_3$ structure has a tolerance factor (t) of 0.82, and for pure $CsMnCl_3$, t is 0.99. Therefore, Mn^{2+} can increase the phase stability of the $CsPbCl_3$ crystallite. While proton radiation can displace H atoms in organic cations, the effect is negligible due to the self-healing mechanism.

In engineering design, annealing effects can be leveraged for in-orbit repair of displacement damage. Equal temperature interval annealing and equal time interval annealing have been shown to decrease the concentration of displacement defects.[81] Heat treatment can extend the lifetime during radiation, and annealing can restore the performance of certain radiation-damaged devices. When designing spacecraft solar cells, it is crucial to incorporate a safety margin to account for displacement damage. This can involve considering the attenuation of V_{OC} and J_{SC} in the calculation of the spacecraft's power requirements, ensuring that the consequences of displacement damage are not severe.

5. Conclusions and future perspectives

This review provides an overview of the space environment and its effects on PSCs. PSCs can be a solution for space PV due to their high power-to-weight ratio and low cost. Additionally, PSCs demonstrate resistance to various space radiations, making them more competitive compared to conventional PV materials. However, for practical application in space, PSCs must withstand challenging environmental conditions and fulfill specific requirements. By developing a thorough understanding of radiation damage mechanisms, targeted measures can be implemented to minimize the adverse effects of radiation on PSCs, thereby enhancing their potential for space applications. For future research, the following perspectives can be taken to promote the space applications of PSCs from infancy to pragmatic applications:

Firstly, the foremost issue is enhancing long-term stability. While PSCs offer advantages in terms of cost and weight, their lifetime is considerably shorter than Si and GaAs cells (~20 years). Fortunately, the absence of moisture and oxygen in space eliminates the concerns regarding the decomposition of MHPs. Therefore, it is imperative to study and improve their radiation stability and thermal stability. Energetic radiation particles cause ionization damage and displacement damage in semiconductor materials, leading to an increase in lattice defects and degradation of PV performance. Understanding the radiation damage mechanism, studying the effect of radiation on each layer, and performing a comprehensive assessment of the complete device is essential to study the degradation of in-orbit performance. Therefore, it is necessary to strengthen the research and develop reasonable stability assessment methods to further improve the radiation resistance of PSCs.

Secondly, the establishment of a comprehensive experimental platform is necessary. Due to the high cost of space launches, most experiments are limited to ground-based laboratories. Many factors in space have a combined effect on PSCs. Current research has only studied them separately and few have simulated environments with multiple factors. A comprehensive experimental platform can help us test, compare, and optimize thoroughly and screen the optimal space PV materials from the perovskite materials such as organic cationic perovskite, all-inorganic perovskite, and double perovskite, enhancing the potential of PSCs to be deployed in space.

Thirdly, a suitable package structure for space applications needs to be designed. Packaging designed for space environments must effectively address challenges such as high vacuum and radiation. Using protective layers to block particle radiation and absorb UV radiation can effectively improve the stability of PSCs. Of course, it is imperative for the protective layer to be lightweight while still maintaining its efficacy. Additionally, the conversion of high-energy radiation into visible light, as previously mentioned, presents an opportunity to simultaneously reduce radiation levels and enhance efficiency. There is also a need for flexible substrates, as they allow for easy deployment through shape alteration and contribute to the reduction of space launch costs by minimizing weight.

Lastly, more experiments in the real space environment are needed. Ground-based experiments merely serve as simulations, lacking the authenticity of real space environments to confirm the viability of PSCs. Currently, there are very few space experiments on PSCs.[83,84] As space technology advances and the demand for next-generation space solar cells grows, it is anticipated that more launch experiments will be conducted to explore the deployment of PSCs in space.

Author contributions

Z. Huan, Y. Zheng and Y. Shao scoped the review, determined the structure and conceptualized the main content. The full text was mainly written by Z. Huan, and the manuscript was critically reviewed and revised by Y. Zheng, K. Wang, W. Ni and J. Zu. Z. Shen provided data and solutions for the space radiation engineering component. J. Zu and Y. Shao provided an overall guidance of the manuscript.

Conflicts of interest

The authors declare that they have no known competing financial interests or personal relationships.

Acknowledgements

This work is supported by the National Natural Science Foundation of China (62104234, 11975052 and 52103279) and the Shanghai Sailing Program (21YF1454000).

Notes and references

1 H. Fujiwara, in *Hybrid Perovskite Solar Cells*, 2021, pp. 1–27, DOI: 10.1002/9783527825851.ch1.
2 A. Kojima, K. Teshima, Y. Shirai and T. Miyasaka, *J. Am. Chem. Soc.*, 2009, **131**, 6050–6051.
3 H.-S. Kim, C.-R. Lee, J.-H. Im, K.-B. Lee, T. Moehl, A. Marchioro, S.-J. Moon, R. Humphry-Baker, J.-H. Yum, J. E. Moser, M. Grätzel and N.-G. Park, *Sci. Rep.*, 2012, **2**, 591.
4 M. Liu, M. B. Johnston and H. J. Snaith, *Nature*, 2013, **501**, 395–398.
5 H. Zhou, Q. Chen, G. Li, S. Luo, T.-b. Song, H.-S. Duan, Z. Hong, J. You, Y. Liu and Y. Yang, *Science*, 2014, **345**, 542–546.
6 W. S. Yang, J. H. Noh, N. J. Jeon, Y. C. Kim, S. Ryu, J. Seo and S. I. Seok, *Science*, 2015, **348**, 1234–1237.
7 Q. Jiang, Y. Zhao, X. Zhang, X. Yang, Y. Chen, Z. Chu, Q. Ye, X. Li, Z. Yin and J. You, *Nat. Photonics*, 2019, **13**, 460–466.
8 H. Min, M. Kim, S.-U. Lee, H. Kim, G. Kim, K. Choi, J. H. Lee and S. I. Seok, *Science*, 2019, **366**, 749–753.
9 H. Min, D. Y. Lee, J. Kim, G. Kim, K. S. Lee, J. Kim, M. J. Paik, Y. K. Kim, K. S. Kim, M. G. Kim, T. J. Shin and S. Il Seok, *Nature*, 2021, **598**, 444–450.
10 NREL, *Best Research-Cell Efficiency Chart*, https://www.nrel.gov/pv/cell-efficiency.html, accessed November, 2023.
11 W. Shockley and H. J. Queisser, *J. Appl. Phys.*, 1961, **32**, 510–519.
12 Y. G. Tu, J. Wu, G. N. Xu, X. Y. Yang, R. Cai, Q. H. Gong, R. Zhu and W. Huang, *Adv. Mater.*, 2021, **33**, 2006545.
13 A. W. Y. Ho-Baillie, H. G. J. Sullivan, T. A. Bannerman, H. P. Talathi, J. Bing, S. Tang, A. Xu, D. Bhattacharyya, I. H. Cairns and D. R. McKenzie, *Adv. Mater. Technol.*, 2021, **7**, 2101059.
14 M. Kaltenbrunner, G. Adam, E. D. Glowacki, M. Drack, R. Schwodiauer, L. Leonat, D. H. Apaydin, H. Groiss, M. C. Scharber, M. S. White, N. S. Sariciftci and S. Bauer, *Nat. Mater.*, 2015, **14**, 1032–1039.
15 N. Aristidou, I. Sanchez-Molina, T. Chotchuangchutchaval, M. Brown, L. Martinez, T. Rath and S. A. Haque, *Angew. Chem., Int. Ed.*, 2015, **54**, 8208–8212.
16 A. R. Kirmani, B. K. Durant, J. Grandidier, N. M. Haegel, M. D. Kelzenberg, Y. M. Lao, M. D. McGehee, L. McMillon-Brown, D. P. Ostrowski, T. J. Peshek, B. Rout, I. R. Sellers, M. Steger, D. Walker, D. M. Wilt, K. T. VanSant and J. M. Luther, *Joule*, 2022, **6**, 1015–1031.
17 V. Romano, A. Agresti, R. Verduci and G. D'Angelo, *ACS Energy Lett.*, 2022, **7**, 2490–2514.
18 J. Yang, Q. Bao, L. Shen and L. Ding, *Nano Energy*, 2020, **76**, 105019.
19 E. G. Stassinopoulos and J. P. Raymond, *Proc. IEEE*, 1988, **76**, 1423–1442.
20 A. Y. Ukhorskiy, M. I. Sitnov, D. G. Mitchell, K. Takahashi, L. J. Lanzerotti and B. H. Mauk, *Nature*, 2014, **507**, 338–340.
21 P. H. Roberts and E. M. King, *Rep. Prog. Phys.*, 2013, **76**, 096801.
22 E. M. King and J. M. Aurnou, *Proc. Natl. Acad. Sci. U. S. A.*, 2015, **112**, 990–994.
23 L. I. Miroshnichenko, *Phys.-Usp.*, 2018, **61**, 323.
24 S. Bourdarie and M. Xapsos, *IEEE Trans. Nucl. Sci.*, 2008, **55**, 1810–1832.
25 T. Robert, K. Andre, M. Chiaki and W. David, *Can. Med. Assoc. J.*, 2009, **180**, 1216–1220.
26 D. R. Taeusch, G. R. Carignan and C. A. Reber, *J. Geophys. Res.*, 1971, **76**, 8318–8325.
27 H. Trinks, K. H. Fricke, U. Laux, G. W. Prölss and U. von Zahn, *J. Geophys. Res.*, 1975, **80**, 4571–4575.
28 J. Yang, Q. Hong, Z. Yuan, R. Xu, X. Guo, S. Xiong, X. Liu, S. Braun, Y. Li, J. Tang, C. Duan, M. Fahlman and Q. Bao, *Adv. Opt. Mater.*, 2018, **6**, 1800262.
29 C. P. Mark and S. Kamath, *Space Policy*, 2019, **47**, 194–206.
30 X. Zhao, M. R. Emami and S. Zhang, *Acta Astronaut.*, 2021, **179**, 56–68.
31 N. Vana, M. Hajek, T. Berger, M. Fugger and P. Hofmann, *Radiat. Prot. Dosim.*, 2006, **120**, 405–409.
32 S. El-Jaby and R. B. Richardson, *Life Sci. Space Res.*, 2015, **6**, 1–9.
33 M. Pugliese, V. Bengin, M. Casolino, V. Roca, A. Zanini and M. Durante, *Radiat. Environ. Biophys.*, 2010, **49**, 359–363.
34 G. Cellere and A. Paccagnella, *IEEE Trans. Device Mater. Reliab.*, 2004, **4**, 359–370.
35 Z. Shen, in *Engineering of the Space Radiation Environment*, ed. X. Cao and J. Yang, China Astronautic Publishing House, Beijing, 2013, pp. 120–159.
36 Z. Li, Y. Zhao, X. Wang, Y. Sun, Z. Zhao, Y. Li, H. Zhou and Q. Chen, *Joule*, 2018, **2**, 1559–1572.
37 G. Grancini, C. Roldan-Carmona, I. Zimmermann, E. Mosconi, X. Lee, D. Martineau, S. Narbey, F. Oswald, F. De Angelis, M. Graetzel and M. K. Nazeeruddin, *Nat. Commun.*, 2017, **8**, 15684.
38 Z. Yang, W. Zhang, S. Wu, H. Zhu, Z. Liu, Z. Liu, Z. Jiang, R. Chen, J. Zhou, Q. Lu, Z. Xiao, L. Shi, H. Chen,

L. K. Ono, S. Zhang, Y. Zhang, Y. Qi, L. Han and W. Chen, *Sci. Adv.*, 2021, **7**, e3749.
39 X. Zhao, T. Liu, Q. C. Burlingame, T. Liu, R. Holley, G. Cheng, N. Yao, F. Gao and Y.-L. Loo, *Science*, 2022, **377**, 307–310.
40 H. Zhu, S. Teale, M. N. Lintangpradipto, S. Mahesh, B. Chen, M. D. McGehee, E. H. Sargent and O. M. Bakr, *Nat. Rev. Mater.*, 2023, **8**, 569–586.
41 M. Yamaguchi, S. J. Taylor, S. Matsuda and O. Kawasaki, *Appl. Phys. Lett.*, 1996, **68**, 3141–3143.
42 B. Cho, J. Davis, L. Hise, A. Korostyshevsky, G. Smith, A. V. Ley, P. Sharps, T. Varghese and M. Stan, in *2009 34th IEEE Photovoltaic Specialists Conference (PVSC)*, Philadelphia, PA, USA, 2009, pp. 001009–001014.
43 Y. Miyazawa, M. Ikegami, T. Miyasaka, T. Ohshima, M. Imaizumi and K. Hirose, in *2015 IEEE 42nd Photovoltaic Specialist Conference (PVSC)*, New Orleans, LA, USA, 2015, pp. 1–4.
44 Y. Miyazawa, M. Ikegami, H. W. Chen, T. Ohshima, M. Imaizumi, K. Hirose and T. Miyasaka, *iScience*, 2018, **2**, 148–155.
45 Z. Song, C. Li, C. Chen, J. McNatt, W. Yoon, D. Scheiman, P. P. Jenkins, R. J. Ellingson, M. J. Heben and Y. Yan, *J. Phys. Chem. C*, 2019, **124**, 1330–1336.
46 C. Xiao, Z. Li, H. Guthrey, J. Moseley, Y. Yang, S. Wozny, H. Moutinho, B. To, J. J. Berry, B. Gorman, Y. Yan, K. Zhu and M. Al-Jassim, *J. Phys. Chem. C*, 2015, **119**, 26904–26911.
47 S. Chen, X. Zhang, J. Zhao, Y. Zhang, G. Kong, Q. Li, N. Li, Y. Yu, N. Xu, J. Zhang, K. Liu, Q. Zhao, J. Cao, J. Feng, X. Li, J. Qi, D. Yu, J. Li and P. Gao, *Nat. Commun.*, 2018, **9**, 4807.
48 A. R. Milosavljevic, W. Huang, S. Sadhu and S. Ptasinska, *Angew. Chem., Int. Ed.*, 2016, **55**, 10083–10087.
49 Z. Dang, J. Shamsi, F. Palazon, M. Imran, Q. A. Akkerman, S. Park, G. Bertoni, M. Prato, R. Brescia and L. Manna, *ACS Appl. Nano Mater.*, 2017, **11**, 2124–2132.
50 T. Sumita, M. Imaizumi, S. Matsuda, T. Ohshima, A. Ohi and H. Itoh, *Nucl. Instrum. Methods Phys. Res., Sect. B*, 2003, **206**, 448–451.
51 A. Jasenek, U. Rau, K. Weinert, H. W. Schock and J. H. Werner, in *Proceedings of 3rd World Conference on Photovoltaic Energy Conversion*, Osaka, Japan, 2003, vol. 1, pp. 593–598.
52 T. Markvart, *J. Mater. Sci.: Mater. Electron.*, 1990, **1**, 1–12.
53 F. Lang, N. H. Nickel, J. Bundesmann, S. Seidel, A. Denker, S. Albrecht, V. V. Brus, J. Rappich, B. Rech, G. Landi and H. C. Neitzert, *Adv. Mater.*, 2016, **28**, 8726–8731.
54 F. Lang, M. Jošt, J. Bundesmann, A. Denker, S. Albrecht, G. Landi, H.-C. Neitzert, J. Rappich and N. H. Nickel, *Energy Environ. Sci.*, 2019, **12**, 1634–1647.
55 R. A. Street, J. E. Northrup and B. S. Krusor, *Phys. Rev. B: Condens. Matter Mater. Phys.*, 2012, **85**, 205211.
56 N. H. Nickel, F. Lang, V. V. Brus, O. Shargaieva and J. Rappich, *Adv. Electron. Mater.*, 2017, **3**, 1700158.
57 F. Lang, O. Shargaieva, V. V. Brus, J. Rappich and N. H. Nickel, *Appl. Phys. Lett.*, 2018, **112**, 081102.
58 D. R. Ceratti, Y. Rakita, L. Cremonesi, R. Tenne, V. Kalchenko, M. Elbaum, D. Oron, M. A. C. Potenza, G. Hodes and D. Cahen, *Adv. Mater.*, 2018, **30**, 1706273.
59 D. Meggiolaro, S. G. Motti, E. Mosconi, A. J. Barker, J. Ball, C. Andrea Riccardo Perini, F. Deschler, A. Petrozza and F. De Angelis, *Energy Environ. Sci.*, 2018, **11**, 702–713.
60 W. S. Yang, B.-W. Park, E. H. Jung, N. J. Jeon, Y. C. Kim, D. U. Lee, S. S. Shin, J. Seo, E. K. Kim, J. H. Noh and S. I. Seok, *Nature*, 2017, **356**, 1376–1379.
61 A. G. Boldyreva, L. A. Frolova, I. S. Zhidkov, L. G. Gutsev, E. Z. Kurmaev, B. R. Ramachandran, V. G. Petrov, K. J. Stevenson, S. M. Aldoshin and P. A. Troshin, *J. Phys. Chem. Lett.*, 2020, **11**, 2630–2636.
62 M. F. Bartusiak and J. Becher, *Appl. Opt.*, 1979, **18**, 3342–3346.
63 S. Yang, Z. Xu, S. Xue, P. Kandlakunta, L. Cao and J. Huang, *Adv. Mater.*, 2019, **31**, e1805547.
64 W. Bannoob, S. M. Ali and S. Aldawood, *Radiat. Phys. Chem.*, 2023, **202**, 110538.
65 K. Yang, K. Huang, X. Li, S. Zheng, P. Hou, J. Wang, H. Guo, H. Song, B. Li, H. Li, B. Liu, X. Zhong and J. Yang, *Org. Electron.*, 2019, **71**, 79–84.
66 S. W. Lee, S. Kim, S. Bae, K. Cho, T. Chung, L. E. Mundt, S. Lee, S. Park, H. Park, M. C. Schubert, S. W. Glunz, Y. Ko, Y. Jun, Y. Kang, H. S. Lee and D. Kim, *Sci. Rep.*, 2016, **6**, 38150.
67 Y. Wang, Z. Zhang, Y. Lan, Q. Song, M. Li and Y. Song, *Angew. Chem., Int. Ed.*, 2021, **60**, 8673–8677.
68 M. Ouafi, B. Jaber, L. Atourki, R. Bekkari and L. Laânab, *J. Alloys Compd.*, 2018, **746**, 391–398.
69 J. Ji, X. Liu, H. Jiang, M. Duan, B. Liu, H. Huang, D. Wei, Y. Li and M. Li, *iScience*, 2020, **23**, 101013.
70 J. P. Correa Baena, L. Steier, W. Tress, M. Saliba, S. Neutzner, T. Matsui, F. Giordano, T. J. Jacobsson, A. R. Srimath Kandada, S. M. Zakeeruddin, A. Petrozza, A. Abate, M. K. Nazeeruddin, M. Grätzel and A. Hagfeldt, *Energy Environ. Sci.*, 2015, **8**, 2928–2934.
71 B. Roose, J.-P. C. Baena, K. C. Gödel, M. Graetzel, A. Hagfeldt, U. Steiner and A. Abate, *Nano Energy*, 2016, **30**, 517–522.
72 M. M. Tavakoli, F. Giordano, S. M. Zakeeruddin and M. Gratzel, *Nano Lett.*, 2018, **18**, 2428–2434.
73 F. Wan, X. Qiu, H. Chen, Y. Liu, H. Xie, J. Shi, H. Huang, Y. Yuan, Y. Gao and C. Zhou, *Org. Electron.*, 2018, **59**, 184–189.
74 N. Arora, M. I. Dar, S. Akin, R. Uchida, T. Baumeler, Y. Liu, S. M. Zakeeruddin and M. Gratzel, *Small*, 2019, **15**, e1904746.
75 T. Leijtens, G. E. Eperon, S. Pathak, A. Abate, M. M. Lee and H. J. Snaith, *Nat. Commun.*, 2013, **4**, 2885.
76 G. Niu, W. Li, F. Meng, L. Wang, H. Dong and Y. Qiu, *J. Mater. Chem. A*, 2014, **2**, 705–710.
77 W. Li, W. Zhang, S. Van Reenen, R. J. Sutton, J. Fan, A. A. Haghighirad, M. B. Johnston, L. Wang and H. J. Snaith, *Energy Environ. Sci.*, 2016, **9**, 490–498.
78 Z. Song, C. Li, C. Chen, J. McNatt, W. Yoon, D. Scheiman, P. P. Jenkins, R. J. Ellingson, M. J. Heben and Y. Yan, *J. Phys. Chem. C*, 2020, **124**, 1330–1336.

79 D. L. Griscom and E. J. Friebele, *Radiat. Eff.*, 1982, **65**, 63–72.
80 F. Bella, G. Griffini, J.-P. Correa-Baena, G. Saracco, M. Grätzel, A. Hagfeldt, S. Turri and C. Gerbaldi, *Nature*, 2016, **354**, 203–206.
81 Z. Shen, in *Engineering of the Space Radiation Environment*, ed. X. Cao and J. Yang, China Astronautic Publishing House, Beijing, 2013, pp. 419–424.
82 W. Liu, J. Zheng, M. Shang, Z. Fang, K.-C. Chou, W. Yang, X. Hou and T. Wu, *J. Mater. Chem. A*, 2019, **7**, 10912–10917.
83 L. K. Reb, M. Böhmer, B. Predeschly, S. Grott, C. L. Weindl, G. I. Ivandekic, R. Guo, C. Dreißigacker, R. Gernhäuser, A. Meyer and P. Müller-Buschbaum, *Joule*, 2020, **4**, 1880–1892.
84 W. Delmas, S. Erickson, J. Arteaga, M. Woodall, M. Scheibner, T. S. Krause, K. Crowley, K. T. VanSant, J. M. Luther, J. N. Williams, J. McNatt, T. J. Peshek, L. McMillon-Brown and S. Ghosh, *Adv. Energy Mater.*, 2023, **13**, 2203920.